Mechanics of Advanced Composite Structures

Semnan University

journal homepage: http://MACS.journals.semnan.ac.ir

Microwave-Assisted Two-Step Sintering of Al/8wt%TiC Composite Prepared by Powder Metallurgy

H. Goodarzi [a], M. Sobhani [a*], H. Abdolahpour [a]

[a] *Faculty of Materials & Metallurgical Engineering, Semnan University, Semnan, Iran*

KEYWORDS

Al/TiC composites
Microwave sintering
TSS method
Bending strength

ABSTRACT

In this work, two-step sintering (TSS) of Al/8wt%TiC with microwave heating has been performed successfully. The composites were fabricated by uniaxial pressing of mixed Al and TiC powders and subsequent sintering in an argon atmosphere at different sintering schedules. The observational studies show a well-dispersed TiC reinforcement in the Al matrix. According to the results, relative density and strength increased from about 95.5% and 90 MPa to 97% and 100 MPa for sintered composites at 640 °C for 2 h and 600 °C for 10 h with single step sintering by a conventional method, respectively. Also, applying the TSS method enhanced the values from 97% and 101 MPa for conventional TSS (T_1=640, T_2=600 °C) to 98% and 211 MPa for microwave-assisted TSS technique. It can be related to the more effective activation of the surface mechanism during fast microwave heating than the tube furnace dilatory heating. Consequently, decreasing the sintering temperature (T_2) can proceed with densifying mechanisms.

1. Introduction

Aluminum matrix composites (AMCs) containing hard reinforcement oxide particles or carbide show attractive properties such as high specific strength, modulus, stiffness, and better wear resistance than pure aluminum and its alloys [1-3]. Powder metallurgy is a suitable technique to produce AMCs and present the figure of merits to other production techniques like producing high performance, net or near-net-shaped parts that reduce the final products' machining costs [4]. To obtain the dense body of aluminum matrix composites by isothermal sintering technique or conventional sintering has been reported for the last decades. As a novel technique of sintering, microwave heating of these composite has been studied and compared with the traditional sintering method. The increased hardness and mechanical properties have been obtained in all reported cases due to rapid microwave heating [5–8]—for example, aluminum matrix composites with 15 wt.% SiC and 7 wt.% TiC as reinforcement have been fabricated by a microwave sintering process. The obtained results of the sintered composite at 750°C in microwave furnace for relative density, bending strength, and micro-hardness were about 96.3%, 340 MPa, and 192 Vickers, respectively [7]. In another research, the addition of 2wt% TiC nanoparticles to 6061 Al alloy caused to increase in the hardness value to about 1180 MPa. For samples that sintered at 600 °C [9]. However, there is no research on the fabrication of aluminum or other metal matrix composites with the two-step sintering (TSS) method. TSS method was introduced to obtain the nanostructured body of Y_2O_3 by I.-Wei Chen for the first time [10]. In the conventional way of sintering processes, the rapid growth of the grains occurs at the final stage of sintering.

Furthermore, at the elevated temperature of conventional sintering, it prevents achieving a dense microstructure [11]. The density enhancement will be possible without allowing the grains' growth if diffusion mechanisms remain active while the grain boundary migration is stopped. The sample is heated up to an elevated temperature known as T1 and then cooled to the lower temperature T2 with a long soaking time to achieve a full dense body to activate the densifying mechanisms in the TSS method. In the first stage of TSS, if density reaches a critical value of about 80% of its

* Corresponding author. Tel.: +98-23-31532380; Fax: +98-23-31532335
E-mail address: m.sobhani@semnan.ac.ir

DOI: 10.22075/macs.2021.22308.1321
Received 21-01-04; Received in revised form 21-01-17; Accepted 21-04-01

theoretical density, the size of the pores remains smaller than what is to be stable. Therefore, in the second stage of sintering at temperature T_2, the pores can move along the grain boundary and leave the sample by capillary force [12]. TSS has been applied successfully to sinter yttrium aluminum garnet (YAG) particles with a size of about 50 nm. The fabricated YAG ceramics contained a homogeneous microstructure with about 43% transmittance and mean grain size of 6 μm for sintered samples at T_1=1800 °C and T_2=1550 °C for 10 h [13]. The Appling TSS method for sintering of nanocrystalline ZnO kept the grain size smaller than 1 μm. It obtained about 98% theoretical density while the grain size of those sintered by conventional heating was about 4 μm [14]. There are several prosperous reports on the sintering of alumina (Al_2O_3) and yttria tetragonal stabilized zirconia (3Y-TZP) using the TSS method [15, 16]. According to the literature, as an objective in the present study, the TSS behavior of the aluminum-8wt%TiC composites using microwave-assisted heating has been studied and compared with the conventional single step and furnace TSS. Also, the mechanical and sintering behavior of composites at the different conditions of the heating program has been investigated.

2. Experimental procedure

2.1. Materials and methods

Pure Aluminum powder (particle size < 20μm, Merck) was used as the matrix, and 8wt% TiC (particle size <50 μm, Sigma Aldrich) was used as the reinforcement as the primary powders. The powders were milled for 10 hours by a planetary ball mill to obtain an incorporated mixture of the powders and dispersion of the reinforcement. The ball to powder ratio (BPR) was 10:1, and the rotation speed was 200 rpm. The particle size of the aluminum powders is expected due to the work hardening and grain fracture process in mechanical milling [17]. Poly amid cups purged with argon gas and alumina balls with 15 mm diameter were used to minimize the impurities. Also, 1wt% methanol was added to the powders as a process control agent (PCA) during milling. PCA materials prevent excessive cold welding and agglomeration during milling and accelerate the rate of grain fracture [18]. Milled powders were pressed with the uniaxial hydraulic pressing machine and stainless steel die at a pressure of 140 MPa. The rectangular samples size was 4×5×25, which is compatible with the bending test. Table 1 shows the different schedules of times and temperatures condition of sintering. Samples were sintered using a quartz tube furnace in an argon atmosphere. The conventional method with 2 and 10 h of soaking time (C and L), TSS with tube furnace (T), microwave (M), and microwave-assisted TSS (MT) were applied for sintering of the composites. In two-step sintering, first, the temperature of the samples was increased to T_1 with a rate of 10°C/min and immediately cooled to T_2 temperature by increasing the argon flow rate and maintained for 10 hours in T_2.

Microwave sintering was done by a domestic microwave that operates with a frequency of 2.45 GHz. All the samples were placed at the same position in the microwave furnace to avoid the geometric conditions influence of the wave radiation. A silicon carbide crucible was insulated with an aluminum silicate blanket used as a wave susceptor. In the microwave-assisted TSS method, the samples were first heated to 640 °C for 5 minutes and then sintered in a tube furnace under an argon atmosphere for 10 hours.

2.2. Characterization and devices

Phase evaluation of the milled powders was done by X-ray diffraction (XRD) device model: D8 Bruker with the wavelength of 1.54 Å (Cu kα) in the range of 2θ=10-90°. A field emission scanning electron microscope (FESEM) model (MIRA II TESCAN, equipped with Energy-dispersive X-ray spectroscopy (EDS)) was employed for particles distribution and morphological observations of the powders and sintered composites. Also, polished surfaces and fractography of the fracture surfaces of sintered samples were studied. The hardness of the samples was measured by the Vickers hardness method using 2 Kg forces or Vickers scale HV2 (ASTM E92). Five indentations were applied for each sample to the evaluation of the average values of the hardness number. Before the tests, samples were sanded and finely polished with 0.5-micron diamond paste to obtain a mirror-polished surface. The density of composites bars was measured by the Archimedes method in deionized water. The strength of the composite bars was measured using a three-point bending technique according to the ASTM D790. Supported span length and cross-head speed were 15 mm and 0.5 mm/min, respectively. The strengths of the composites were calculated according to the below equations [19]:

$$\sigma = \frac{3PL}{2bh^2} \quad (1)$$

where P is the load, L is the span length of the support. b and h are the width and height of the bars. Five specimens were examined to determine the average value and error bars of the strength of the composite.

Table 1. Times and temperatures of sintering schedule

Sample	Sintering time (Hour)	Sintering temperature (°C)
C580	2	580
C600	2	600
C620	2	620
C640	2	640
C660	2	660
L580	10	580
L600	10	600
L620	10	620
T58-62	10	T_1= 620, T_2= 580
T58-64	10	T_1= 640, T_2= 580
T58-66	10	T_1= 660, T_2= 580
T60-62	10	T_1= 620, T_2= 600
T60-64	10	T_1= 640, T_2= 600
M64	5 min	640
MT60-64	5min – 10h	T_1= 640, T_2= 600

3. Results and discussions

Figure 1 shows the XRD patterns of Al/8wt%TiC composite and pure Al powder. The composite batch was milled for 10 h, and the pure Al powder was without further milling. The patterns indicate that the intensity of diffracted peaks of Al in the composite has been decreased during milling. The significant happening is peak broadening due to the reduction of crystallite sizes of Al powders. The aluminum particles become finer by work hardening and fracture in mechanical milling [20].

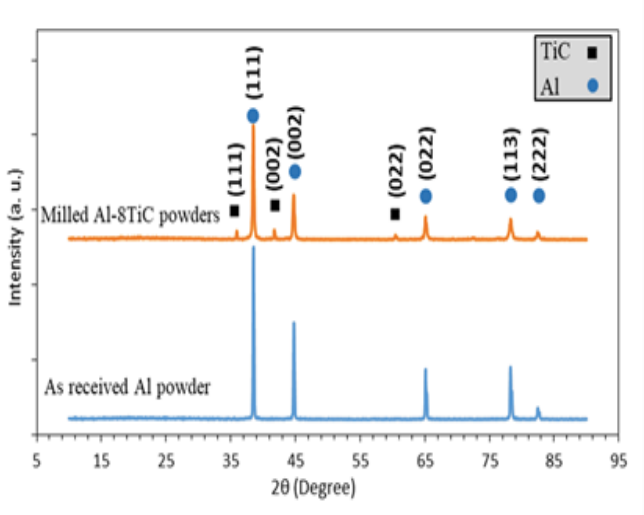

Fig. 1. XRD patterns of pure Al powder and 10 h milled Al/8wt% TiC composite

This process can be accelerated in the presence of external hard impurities such as TiC particles [21]. Both Al and TiC have similar cubic (FCC) crystal structures and have diffraction patterns in similar planes like (111), (002), and (022). Also, the oxide impurities caused by mechanical milling were not observed with XRD analysis accuracy. FE-SEM images of the composite powders milled for 10 hours show the formation of ultra-fine milled particles (Fig. 2). The soft agglomerate can be formed due to the electrostatic force of electrical charge on the surface of the particles. Also, the cold welding of fine metallic particles can lead to the formation of hard agglomerates. However, they have an average size of about 8 microns. Within each of these agglomerates, the laminated nanoparticles attached can be observed. The air atmosphere of the milling cups contains oxygen, so the particles laminate [22].

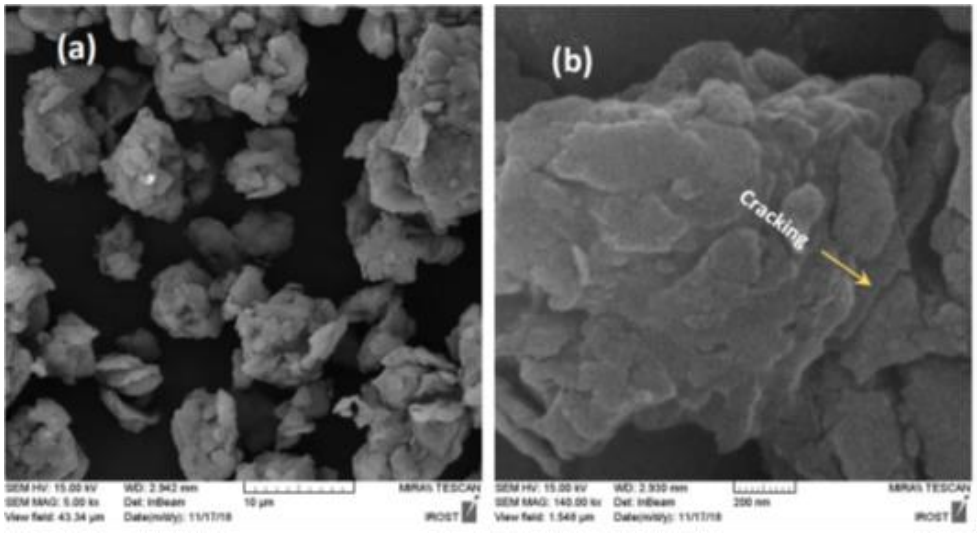

Fig. 2. (a) and (b) FESEM micrograph of the Al/8wt%TiC composite powders milled for 10 hours at different magnifications

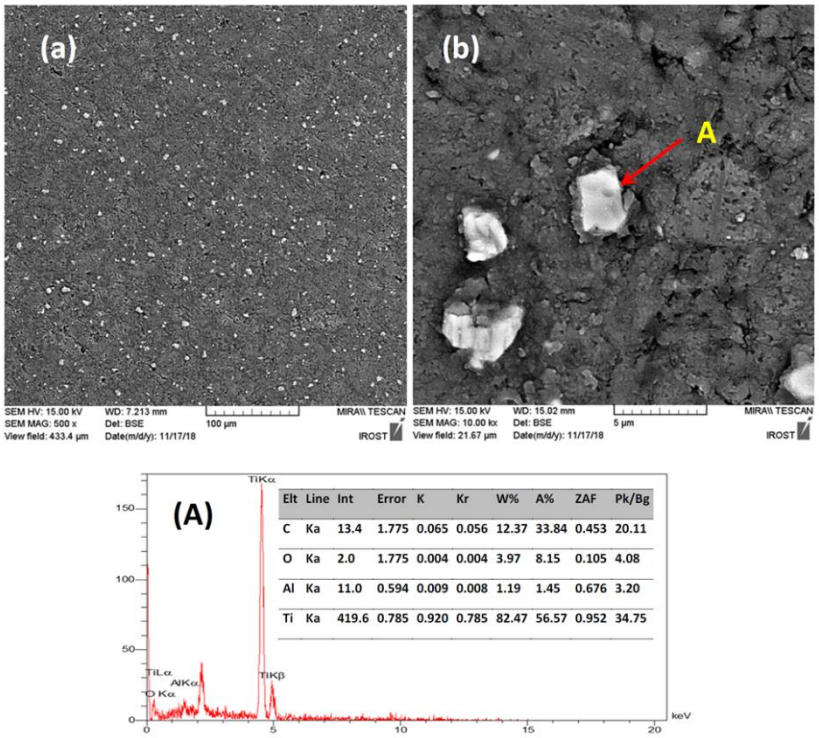

Fig. 3. FESEM micrograph of the Al/8wt%TiC composite sintered at 620° C for 2 h (a, b) with related EDAX of the particle A

Figure 3 shows the sintered sample's backscattered electron (BSE) image at 620° C for 2 h. According to Fig. 3 (a), a well-dispersed microstructure of TiC reinforcement has been obtained in the aluminum matrix. In the BSE mode of SEM, the matrix is darker than the reinforcement. The TiC particles appear lighter due to a higher probability of producing an elastic collision due to the greater atomic mass of Ti than Al. The size of the TiC reinforcement particles is less than 5 microns, as shown by the arrow in Fig. 3 b. Also, the EDAX analysis of the pointed particle A approves the composition to the TiC that contains the Ti and C elements. Figure 4 shows the relative density and hardness variation of the sintered composites samples (C580-C660) at different temperatures with a soaking time of 2 h by the conventional method. The pressed composites' green bar achieved a maximum value of 85% of the theoretical density at the compaction pressure of 140 MPa. During the sintering process, with rising temperature up to 640 °C, the composite sample density increased to about 95% of the theoretical density. It seems approaching the melting point of Al, waking up of the surface sintering mechanisms promote the formation of the spherical pores. It should be mentioned that the surface mechanisms include vapor transport, surface diffusion, and lattice diffusion from the surface, well known as the non-densifying mechanisms. The rounded pores are thermodynamically stable and lead to density loss. Most pores are pined at the grain boundary at the end of the second sintering stage, especially at the three-grain boundary. Since the atomic flux in the grain boundary is higher than the lattice, the pores must remain along the grain boundary and move along them simultaneously during grain growth to disappear. The pore mobility that moves through the surface flux of the atoms can be expressed as [23]:

$$M_p^s = \frac{D_s \delta_s \Omega}{\pi r^4 kT} \propto \frac{1}{r^4} \quad (2)$$

Where: D_s, δ_s‘, Ω, r, k, and T are atomic diffusion coefficient, diffusion thickness, atomic volume, pore radius, Boltzmann constant, and sintering temperature. According to the above equation, the increased sintering temperature caused growth in the formation rate and mobility of the pores due to diffusion coefficient (D_s) increment. Therefore, as the cavities increased mobility, they were separated from the grain boundaries, trapped inside the grains, and became stable. Regarding Fig. 4, the initial increase of the hardness from 580 to 600 °C is related to the condensation and density increment, whereas the grain or pores have not been coarse yet. In the powder sintering process, the hardness is dependent on density and grain size. Achieving a high density may cause an increase in the grain size and consequently decrease the hardness or strength of sintered materials. Therefore, the maximum hardness value for composites sintered for 2h can be obtained before achieving the maximum density value, just before grain size growth at 600-620 °C.

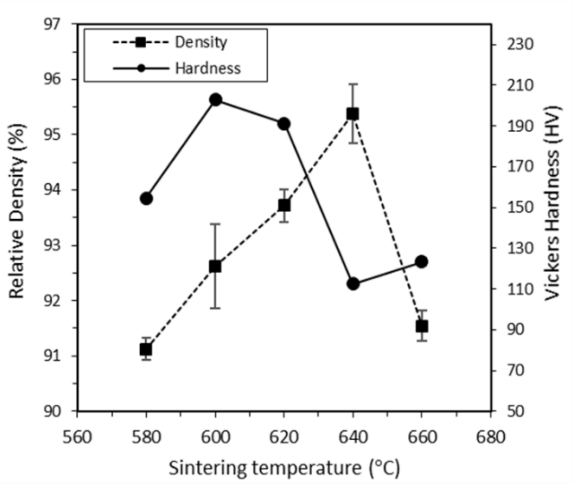

Fig. 4. Hardness and relative density variation of C580-C660 composites with sintering temperature

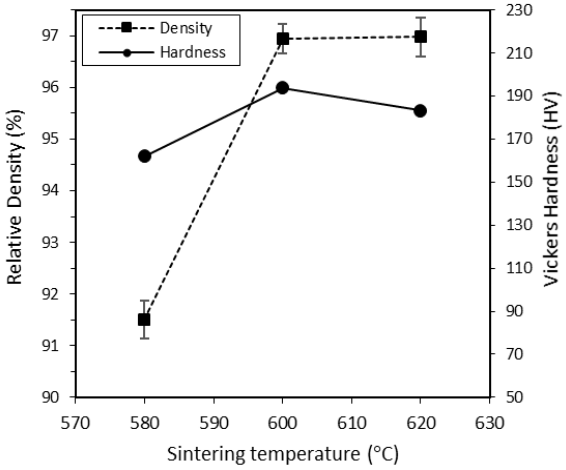

Fig. 5. Hardness and relative density Variation of L580, L600, and L620 composites with sintering temperature.

The soaking time of sintering is considered a long time of 10 h to decrease the grain growth rate and increase the densification. Based on Fig. 5, there is a negligible difference in density and hardness variation between sintered samples at 580 °C for 2 and 10 h. Increasing the sintering time at a low temperature does not provide a suitable atomic diffusion condition for condensation. With increasing the temperature to 600 °C, the density increased to 97% of the theoretical density.

Also, the specimen L600 hardness increased compared to the L580, and it is not much lower than the sintered specimen at the same temperature for 2 h. Further rising temperature to 620 °C doesn't cause an increase in the density, and the rising temperature effect cause to decrease in the hardness from about 190 to 180 (HV). In brief, the densities of the samples at two temperatures of 600 and 620 °C varied with time, while the hardness of specimens did not change significantly. Calculated strengths of the sintered samples C and L series, using Eq. 1, are presented in Fig. 6. It shows the strengths of all samples versus temperature at two different soaking times 2 (dashed line) and 10 (solid line) hours. As mentioned above, diffusion paths among the grains were not made to increase the density at 580 °C and the sintered samples for 2 or 10 hours did not withstand bending. The three-point bending test results correspond to the density and hardness tests in Figures 5 and 6. Following the density value, the strength of other sintered samples at 600 and 620 °C has not been raised yet. Further increasing of the temperature to 640 °C shows a considerable mutation of power during sintering mechanisms activation. With increasing the soaking time of sintering from 2 to 10 h, the strength of the composites significantly increased.

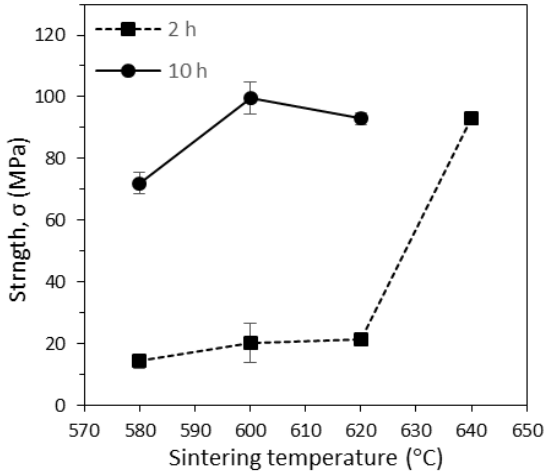

Fig. 6. Bending strength vs. sintering temperatures of 2 and 10 hours sintered composites.

Long time sintering caused to increase in the density followed by the removal of the pores and enhanced the strength of the specimens, consequently. Concerning the Chen report about TSS of ceramics, when ceramic powder samples heated up to their conventional sintering temperature (T_1), the necking stage passed and the diffusion paths formed by non-densifying mechanisms. The most important condition of this stage is achieving the density to above 75% of green density. With consequent cooling to conventional sintering temperature (T_2), condensation can be complete without grain growth in a frozen structure. It is possible because of the differences between the kinetic condition of the grain growth and condensation [10]. The obtained results of the composites sintered with the TSS method (series T) are shown in table 2. According to the T1>620 (C (sample T58-64) results, density decreased during the formation of the stable spherical pores during heating. Therefore, it can be concluded that there is enough time to activate the surface mechanisms at a high temperature of T_1 with

conventional furnace heating. Also, the improvement of the density is possible only by increasing the sintering temperature T_2. Microwave heating was applied for the composites to eliminate the effect of the heating rate on T1.

The results of the composites include microwave heating, which is shown in table 3. Fast heating of the microwave can improve the densification process of the samples. The composites achieved about 97% of theoretical density at T_1=650 °C with a short soaking time of 5 minutes. However, a conventional tube furnace can improve further with post-sintering at lower temperatures (T2). It is a combination of microwave and traditional furnace to develop a corrected TSS method for metal powder sintering in this study.

Table 2. Hardness, relative density, and bending strength of the conventional TSS composites

Sample	Hardness (HV)	Relative density (%)	Bending strength (MPa.)
T58-62	151	91.2	71.2
T58-64	149.2	89.9	72.5
T58-66	143.6	92.4	70.9
T60-62	188.4	96.7	98.9
T60-64	187	96.9	101

Table 3. Relative density and bending strength of the microwave and microwave-assisted TSS composites

Sample	Relative density (%)	Bending strength (MPa.)
MT65-600	98.1	211.5
M65	97.4	162

The results of the three-point bending test (Load-Deflection) of selected sintered samples for 2 and 10 h by conventional and including microwave method are illustrated in Fig. 7. The selected samples have the maximum value of density in the sintering schedule. Suppose the total work or elastic energy stored in the samples (W) is assumed to be related to the surface area under the curve (such as tension test) called. In that case, it can be seen that both of the heated microwave samples have the maximum value. In the case of conventional sintered samples, increasing the sintering time increased the W due to density increasing with long time sintering compared with the samples sintered for 2 h and W_{L620}>W_{L600}> W_{C640}. The microwave-assisted TSS method presents the highest values of strength and density. It reveals that applying fast heating to obtain T_1 is more effective than the conventional TSS, and it satisfies the best condition of the TSS technique. Rapid microwave heating of composite causes necking or grain boundary formation with surface mechanisms at the first stage of sintering in the shortest time possible. Hence, the second or main condensation stage can act useful at lower temperature T_2 with conventional heating.

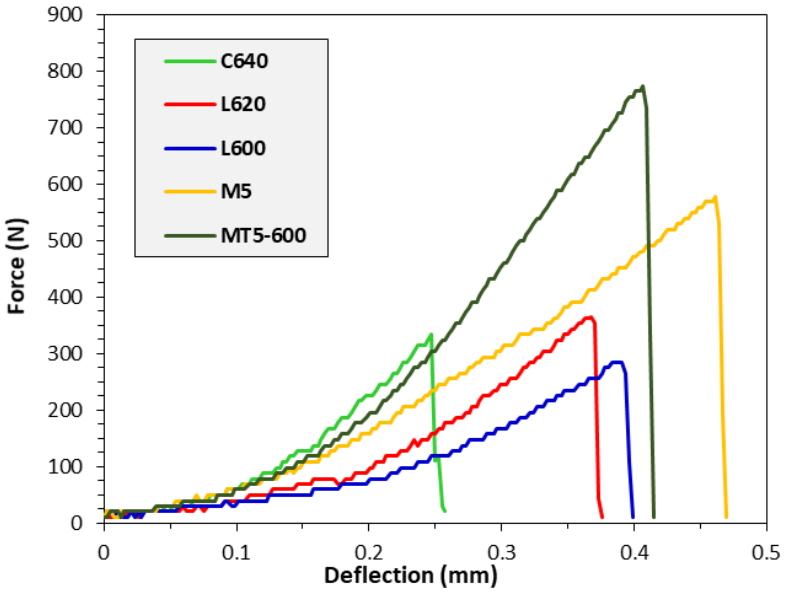

Fig. 7. Force vs. deflection variation of sintered composites.

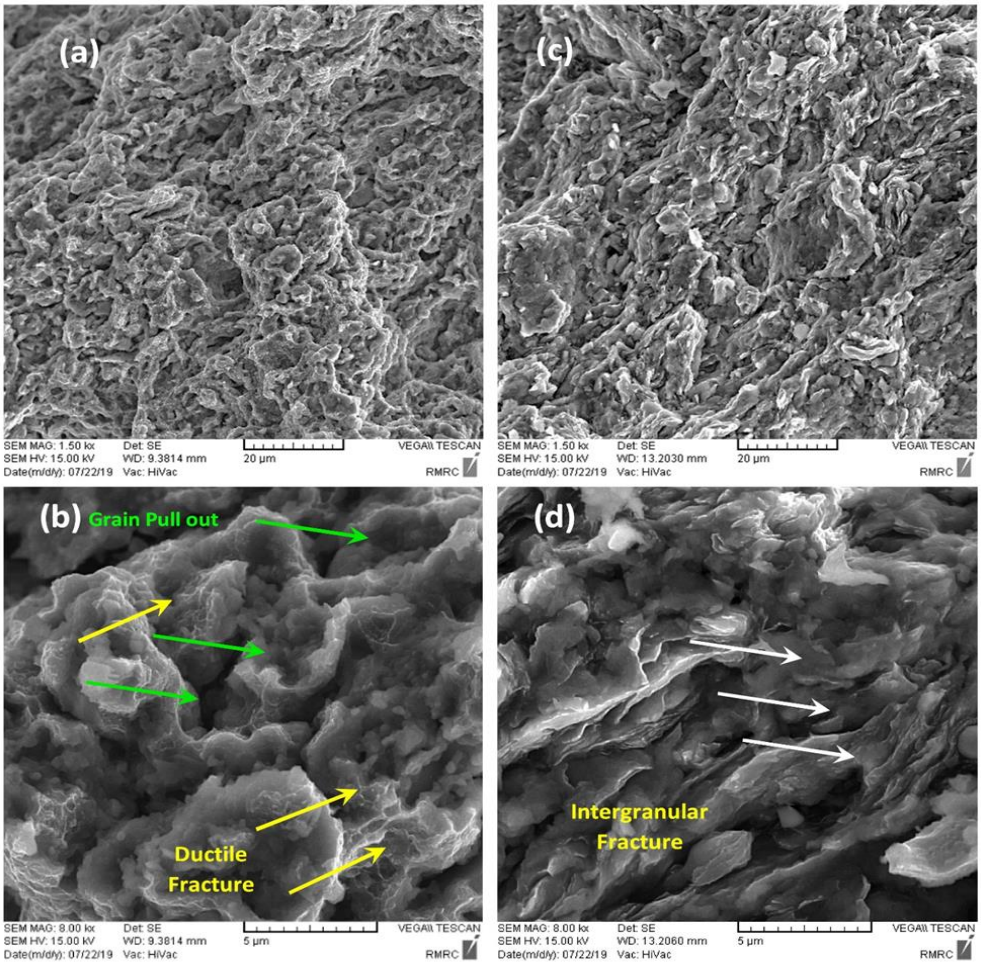

Fig. 8. SEM image of fracture surface MT5-600 (a,b) and L620 (c,d) composites.

Figure 8 shows the fracture surfaces of the MT5-600 and L620 composites. According to the image, it can be seen that there is some plastic deformation in the fracture surface of MT5-600 (Fig. 8-a), while for sample L620 the inter-granular separation of the grains without further plastic deformation is observed. Before fracture, the grains' deformation is clearer at high magnification (Fig. 8-b), and ductile zones are indicated with yellow arrows. The increasing strength can also be related to the bridging mechanism of the ductile grains at the crack tip or grain pull out [24], shown with green arrows. Combining the plastic deformation and grain pull-out fracture can be the main cause of the enhanced properties of the composites prepared by the microwave-assisted TSS method.

4. Conclusion

Fabrication of a dispersed microstructure of micronized TiC reinforced Aluminum composites with mechanical milling, and cold pressing has been developed. With increasing the sintering time from 2h to 10h and decreasing the sintering temperature from 640 to 600 °C relative density and strength increased from about 95.5% and 90 MPa to 97% and 100 MPa, respectively single step sintering. Applying the TSS method, values enhanced from about 97% and 101 MPa for conventional TSS (T1=640, T2=600 °C) to 98% and 211 MPa for microwave-assisted TSS technique the more effective activation of the surface mechanism by microwave heating than the conventional dilatory heating. The densifying mechanism can wake up at a lower temperature (T_2) after successfully passing the first stage (T_1) in the microwave-assisted TSS method. Fracture of single-step composites accommodated with inter-granular and the TSS composites is a combination of the plastic deformation and grain pull-out fracture that can be the main cause of the enhancement properties of the composites.

References

[1] Rahimipour, M.R., Sobhani, M., 2013. Evaluation of centrifugal casting process parameters for in situ fabricated functionally gradient Fe-TiC composite. *Metallurgical and Materials Transactions B: Process Metallurgy and Materials Processing Science*, *44*(5), pp.1120–1123.

[2] Albiter, A., León, C.A., Drew, R.A.L., Bedolla, E., 2000. Microstructure and heat-treatment response of Al-2024/TiC composites.

Materials Science and Engineering A, *289*(1), pp.109–115.

[3] Bauri, R., Yadav, D., Suhas, G., 2011. Effect of friction stir processing (FSP) on microstructure and properties of Al-TiC in situ composite. *Materials Science and Engineering A*, *528*(13–14), pp.4732–4739.

[4] Jabbari Taleghani, M.A., Ruiz Navas, E.M., Torralba, J.M., 2014. Microstructural and mechanical characterisation of 7075 aluminum alloy consolidated from a premixed powder by cold compaction and hot extrusion. *Materials and Design*, *55*, pp.674–682.

[5] Ghasali, E., Alizadeh, M., Ebadzadeh, T., Pakseresht, A.H., Rahbari, A., 2015. Investigation on microstructural and mechanical properties of B_4C-aluminum matrix composites prepared by microwave sintering. *Journal of Materials Research and Technology*, *4*(4), pp.411–415.

[6] Ghasali, E., Pakseresht, A.H., Agheli, M., Marzbanpour, A.H., Ebadzadeh, T., 2015. WC-co particles reinforced aluminum matrix by conventional and microwave sintering. *Materials Research*, *18*(6), pp.1197–1202.

[7] Ghasali, E., Yazdani-rad, R., Asadian, K., Ebadzadeh, T., 2017. Production of Al-SiC-TiC hybrid composites using pure and 1056 aluminum powders prepared through microwave and conventional heating methods. *Journal of Alloys and Compounds*, *690*, pp.512–518.

[8] Verma, J., Kumar, A., Chandrakar, R., Kumar, R., 2012. Processing of 5083 Aluminum Alloy Reinforced with Alumina through Microwave Sintering. *Journal of Minerals and Materials Characterization and Engineering*, *11*(11), pp.1126–1131.

[9] Jeyasimman, D., Sivasankaran, S., Sivaprasad, K., Narayanasamy, R., Kambali, R.S., 2014. An investigation of the synthesis, consolidation and mechanical behaviour of Al 6061 nanocomposites reinforced by TiC via mechanical alloying. *Materials and Design*, *57*, pp.394–404.

[10] Chen, I.W., Wang, X.H., 2000. Sintering dense nanocrystalline ceramics without final-stage grain growth. *Nature*, *404*(6774), pp.168–171.

[11] Sobhani, M., Ebadzadeh, T., Rahimipour, M.R., 2014. Formation and densification behavior of reaction sintered alumina-20 wt.% aluminium titanate nano-composites. *International Journal of Refractory Metals and Hard Materials*, *47*, pp.49–53.

[12] Mazaheri, M., Valefi, M., Hesabi, Z.R., Sadrnezhaad, S.K., 2009. Two-step sintering of nanocrystalline $8Y_2O_3$ stabilized ZrO_2 synthesized by glycine nitrate process. *Ceramics International*, *35*(1), pp.13–20.

[13] Chen, Z. hui, Li, J. tao, Xu, J. jun, Hu, Z. gui. , 2008. Fabrication of YAG transparent ceramics by two-step sintering. *Ceramics International*, *34*(7), pp.1709–1712.

[14] Mazaheri, M., Zahedi, A.M., Sadrnezhaad, S.K., 2008. Two-step sintering of nanocrystalline ZnO compacts: Effect of temperature on densification and grain growth. *Journal of the American Ceramic Society*, *91*(1), pp.56–63.

[15] Wang, C.J., Huang, C.Y., Wu, Y.C., 2009. Two-step sintering of fine alumina-zirconia ceramics. *Ceramics International*, *35*(4), pp.1467–1472.

[16] Mazaheri, M., Simchi, A., Golestani-Fard, F., 2008. Densification and grain growth of nanocrystalline 3Y-TZP during two-step sintering. *Journal of the European Ceramic Society*, *28*(15), pp.2933–2939.

[17] Afkham, Y., Khosroshahi, R.A., Kheirifard, R., 2017. Microstructure and Morphological Study of Ball-Milled Metal Matrix Nanocomposites 1, *118*(8), pp.749–758.

[18] Suryanarayana, C., 2001. Mechanical Alloying and Milling Mechanical Engineering. *Progress in Materials Science*, *46*, pp.1–184.

[19] Vaziri, P., Balak, Z., 2019. Improved mechanical properties of ZrB_2-30 vol% SiC using zirconium carbide additive. *International Journal of Refractory Metals and Hard Materials*, *83*(April), pp.104958.

[20] Hesabi, Z.R., Simchi, A., Reihani, S.M.S., 2006. Structural evolution during mechanical milling of nanometric and micrometric Al_2O_3 reinforced Al matrix composites. *Materials Science and Engineering A*, *428*(1–2), pp.159–168.

[21] Abdoli, H., Asgharzadeh, H., Salahi, E., 2009. Sintering behavior of Al-AlN-nanostructured composite powder synthesized by high-energy ball milling. *Journal of Alloys and Compounds*, *473*(1–2), pp.116–122.

[22] Ramezani, M., Neitzert, T., 2012. Mechanical milling of aluminum powder using planetary ball milling process. *Journal of Achievements in Materials and Manufacturing Engineering*, *55*(2), pp.790–798.

[23] Suk-Joong L.Kang. , 2005. *Sintering Densification,Grain Growth,and Microstructure*. *Elsevier Butterworth-Heinemann Linacre House*.

[24] Karimirad, S., Balak, Z., 2019. Characteristics of spark plasma sintered ZrB_2-SiC-SCFs composites. *Ceramics International*, *45*(5), pp.6275–6281.